



# Removal of zirconium from aqueous solution by modified clinoptilolite

H. Faghihian\*, M. Kabiri-Tadi

Department of Chemistry, University of Isfahan, 81746-73441, Isfahan, Iran

## ARTICLE INFO

### Article history:

Received 24 May 2009

Received in revised form 2 January 2010

Accepted 9 January 2010

Available online 18 January 2010

### Keywords:

Zirconium  
Clinoptilolite  
Adsorption

## ABSTRACT

Adsorptive behavior of natural clinoptilolite was assessed for the removal of zirconium from aqueous solutions. Natural zeolite was characterized by X-ray diffraction, X-ray fluorescence, thermal methods of analysis and FTIR. The zeolite sample composed mainly of clinoptilolite and presented a cation exchange capacity of  $1.46 \text{ meq g}^{-1}$ . K, Na and Ca-exchanged forms of zeolite were prepared and their sorption capacities for removal of zirconium from aqueous solutions were determined. The effects of relevant parameters, including initial concentration, contact time, temperature and initial pH on the removal efficiency were investigated in batch studies. The pH strongly influenced zirconium adsorption capacity and maximal capacity was obtained at pH 1.0. The maximum removal efficiency obtained at  $40^\circ\text{C}$  and equilibration time of 24 h on the Ca-exchanged form. Kinetics and isotherm of adsorption were also studied. The pseudo-first-order, pseudo-second-order, Elovich and intra-particle diffusion models were used to describe the kinetic data. The pseudo-second-order kinetic model provided excellent kinetic data fitting ( $R^2 > 0.998$ ) with rate constant of  $1.60 \times 10^{-1}$ ,  $1.96 \times 10^{-1}$ ,  $2.45 \times 10^{-1}$  and  $2.02 \times 10^{-1} \text{ g mmol}^{-1} \text{ min}^{-1}$  respectively for Na, K, Ca-exchanged forms and natural clinoptilolite. The Langmuir and Freundlich models were applied to describe the equilibrium isotherms for zirconium uptake and the Langmuir model agrees very well with experimental data. Thermodynamic parameters were determined and are discussed.

© 2010 Elsevier B.V. All rights reserved.

## 1. Introduction

Zirconium is a significant engineering material and has become important as secondary metal for carrying out certain kind of industrial processes such as manufacturing of photoflash bulbs, surgical equipments, and tanning of leather. Despite its ability to be used for many different industrial applications, most of the zirconium produced today is used in water-cooled nuclear reactors. Pure zirconium metal can be produced by ductile process which is too expensive for general use. Thus once in solution it is of great importance if zirconium can be selectively adsorbed from its solution [1,2].

Several methods for separation of zirconium from liquid solution including precipitation, using of organic and inorganic reagents, liquid–liquid extraction, chromatography, extraction chromatography, cation exchange chromatography, reversed-phase chromatography and ion exchange have been reported [2–8]. Dosch and Conrad described a cation exchange procedure for quantitative separation of zirconium and titanium from each other by Dowex AG 50-W-X8 [9]. Qureshi and Husain performed quantitative cation exchange separation of zirconium and hafnium in formic

acid media by Dowex 50W-X8 [10]. Larsen and Wang have studied the ion exchange separation of zirconium and hafnium in perchloric acid with Amberlite IR-120 [11]. Zhang et al. prepared silica gel with high specific surface area and high adsorption activity and separated zirconium selectively in simulated high level radioactive liquid waste [1]. Yang et al. used a supported liquid membrane system for separation of zirconium and hafnium [12,13]. Removal and recovery of zirconium from dilute aqueous solutions by *Candida tropicalis* (a biosorbent) has been done [2]. Dyer and Kadhim studied the removal of zirconium by clinoptilolite [14].

A Zeolite is crystalline aluminosilicate with a three-dimensional framework structure that forms uniformly sized pores of molecular dimensions. As the pores preferentially adsorb species that fit snugly inside the pores and exclude species that are too large, they act as sieves on a molecular scale. Zeolites' structure consists of robust, crystalline silica frameworks. At some places in the framework  $\text{Al}^{3+}$  has replaced  $\text{Si}^{4+}$  and the framework carries a negative charge. Loosely held cations that sit within the cavities preserve the electroneutrality of the zeolite. Some of these cations are amenable to cation exchange. The aluminosilicate structure of zeolites makes them very stable against radioactive radiation [15]. The sorption on zeolitic particles is a complex process because of their porous structure, inner and outer charged surfaces, mineralogical, existence of crystal edges, broken bands and other imperfections of the surface [16]. The reason for selecting zeolite as an adsorbent is its relatively

\* Corresponding author. Tel.: +98 311 7932700; fax: +98 311 6689732.  
E-mail address: [h.faghih@sci.ui.ac.ir](mailto:h.faghih@sci.ui.ac.ir) (H. Faghihian).

moderate surface area, high and selective ion exchange capacity, low cost and relative simplicity of application and operation [15].

Clinoptilolite is the most abundant natural zeolite and its typical unit cell formula is given either as  $\text{Na}_6[(\text{AlO}_2)_6(\text{SiO}_2)_{30}]\cdot 24\text{H}_2\text{O}$  or  $(\text{Na}_2, \text{K}_2, \text{Ca}, \text{Mg})_3[(\text{AlO}_2)_6(\text{SiO}_2)_{30}]\cdot 24\text{H}_2\text{O}$  [17,18].

The aim of this work was to study the efficiency of natural and cation exchanged forms of clinoptilolite for removal of zirconium from aqueous solutions. The effect of different parameters such as initial concentration, initial pH of the solution, contact time and temperature on adsorption process is also studied. Kinetic and thermodynamic parameters of the process are calculated.

## 2. Experimental

All chemical reagents used in this study were of analytical reagent grade (AR Grade). All solutions were prepared in double distilled water. Solutions of zirconium were prepared by dissolving 2.6067 g zirconium tetrachloride ( $\text{ZrCl}_4$ ) in 1000 mL distilled water. pH value of this solution was 1.85. The pH was adjusted by addition of HCl and NaOH.

Natural clinoptilolite was collected from Semnan deposits in Iran. It was crushed and pulverized in mortar and sieved to a particle size of 224–400  $\mu\text{m}$ . The powder was refluxed in distilled water in order to remove soluble salts then washed and dried at 110 °C. The powder was stored in a desiccator over saturated NaCl solution in order to maintain a constant vapor pressure during the whole period of the experiments. The purified sample was characterized by X-ray diffraction, FTIR and thermal method of analysis. X-ray diffraction patterns were taken by a Bruker, D8ADVANCE X-ray diffractometer using  $\text{Cu K}\alpha$  radiation (wavelength: 1.5406 Å and filter: Ni) up to  $2\theta = 45$  at ambient temperature. Scanning parameters are step size = 0.04° and time step = 2 s. ICDD cards were used to identify phases in the zeolite samples. Na, K, Ca, Si, and Al contents of the sample were determined by a Bruker, S4PIONEER X-ray fluorescence spectrometer (XRF). Zeolite samples were prepared as briquettes. The vacuum mode was used for recording XRF spectra of samples. FTIR spectrum of the clinoptilolite was obtained by a Nicolet Impact 400D Model spectrophotometer (Nicolet Impact, Madison, USA) using the KBr pressed disk technique. For KBr pellet, 1 mg of zeolite and 100 mg of KBr were weighted, ground in an agate mortar, and pressed. Spectrum was recorded in the wave number range from 400 to 4000  $\text{cm}^{-1}$ . Thermogravimetric analysis was performed using Mettler, TG-50 thermal analyzer from ambient temperature to 800 °C in air condition.

Cation exchange capacity (CEC) of clinoptilolite was measured by dispersion of purified clinoptilolite in 1 mol L<sup>-1</sup>  $\text{NH}_4\text{NO}_3$  solution with liquid to solid ratio of 20:1 and shaken for 72 h. After that, the suspension was centrifuged and the amount of exchanged cations in solution was measured by Shimadzu AA-670 atomic absorption spectrometer. The experimental CEC was considered as the sum of meq of  $\text{Na}^+$ ,  $\text{K}^+$ ,  $\text{Ca}^{2+}$  and  $\text{Mg}^{2+}$  in the solution for 1 g of zeolite [19].

The theoretical exchange capacity (TCEC) is characteristic for given zeolitic materials. It can be from its chemical composition as a sum of exchangeable ions ( $\text{Na}^+$ ,  $\text{K}^+$ ,  $\text{Mg}^{2+}$ , and  $\text{Ca}^{2+}$ ) present in 1 g of zeolite [20]. It is obvious that same of the exchangeable cations do not necessarily have the ion-exchange ability [21]. So the experimental CEC is usually lower than TCEC. In this research TCEC values were calculated from the chemical composition of the samples obtained by the XRF technique (Table 1).

To prepare the exchanged forms of clinoptilolite 5 g of the purified zeolite was shaken with 100 mL solution of 1 mol L<sup>-1</sup>  $\text{NH}_4\text{Cl}$  at 60 °C for 72 h. The solid was filtered, washed and dried at 110 °C. This solid is  $\text{NH}_4^+$ -form of clinoptilolite. The H-form of clinoptilolite was prepared by calcining the  $\text{NH}_4^+$ -form at 450 °C for 2 h to remove ammonia molecule. Na, K and Ca-exchanged forms were prepared

**Table 1**

Chemical composition of the natural and cation exchanged forms of clinoptilolite obtained by XRF method.

wt. (%)				
Species	Clinoptilolite	Na-form	K-form	Ca-form
$\text{SiO}_2$	67.71	70.74	68.30	71.85
$\text{Al}_2\text{O}_3$	11.30	11.40	11.37	12.50
$\text{Na}_2\text{O}$	2.39	3.30	1.52	1.03
CaO	2.09	2.21	0.47	2.91
$\text{K}_2\text{O}$	1.86	0.35	6.23	0.92
MgO	0.696	0.70	0.32	0.53
$\text{Fe}_2\text{O}_3$	0.439	0.68	0.32	0.40
$\text{TiO}_2$	0.116	0.13	0.08	0.12
SrO	0.107	0	0	0.09
BaO	0.059	0	0	0
LOI*	13.2	10.16	11.50	9.60
Total	99.97	99.67	100.11	99.95
Si/Al	5.086	5.270	5.100	4.880

\* Loss on ignition.

by shaking 5 g of H-form of zeolite with 100 mL of 1 mol L<sup>-1</sup> solutions of  $\text{NaNO}_3$ ,  $\text{KNO}_3$  and 0.5 mol L<sup>-1</sup> of  $\text{Ca}(\text{NO}_3)_2$ , respectively, at 60 °C for 72 h. The solid was separated, washed with distilled water, dried at 110 °C, and stored in the desiccator.

Adsorption of zirconium was studied by batch technique. 0.5 g of zeolite was equilibrated with 10 mL of zirconium solution of known concentration at fixed temperature for known period of time. After equilibration, filter-separating of solid phase was followed by centrifuging (3000 rpm for 15 min). A portion of supernatant solution was taken for zirconium measurement using ICP-OES technique (Integra-XL from GBC Company).

The amount of adsorbed zirconium was calculated from the difference of concentrations before and after adsorption.

$$q = (C_i - C_f) \times V/m \quad (1)$$

where  $q$  is the amount of metal ions adsorbed by unit mass of zeolite ( $\text{meq g}^{-1}$ );  $C_i$  and  $C_f$  are respectively initial and final concentrations ( $\text{meq L}^{-1}$ );  $m$  is the amount of zeolite used (g) and  $V$  is the volume of zirconium solution (L).

The effect of different parameters, including initial zirconium concentration, pH of the solution, contact time and temperature was determined by changing one parameter and keeping other parameters constant.

## 3. Results and discussion

### 3.1. Physicochemical characterization

The theoretical and experimental cation exchange capacity of natural and cation exchanged forms of clinoptilolite are presented in Table 2. The difference is attributed to the fact that some of the exchanged sites in the bigger particles are not available for the ingoing cations. It is believed that as the particle size of the zeolite becomes smaller, these values would be more similar. Different CEC for clinoptilolite from various regions in the world have been reported in literature [22–24].

**Table 2**

Comparison of natural and cation exchanged forms of clinoptilolite.

Exchangeable cation	Clinoptilolite	Na-form	K-form	Ca-form
Na	0.77	1.07	0.49	0.33
K	0.40	0.08	1.32	0.20
Ca	0.38	0.39	0.08	0.59
Mg	0.17	0.17	0.08	0.13
TCEC ( $\text{meq g}^{-1}$ )	1.71	1.71	1.97	1.25
CEC ( $\text{meq g}^{-1}$ )	1.46	1.43	1.82	1.20

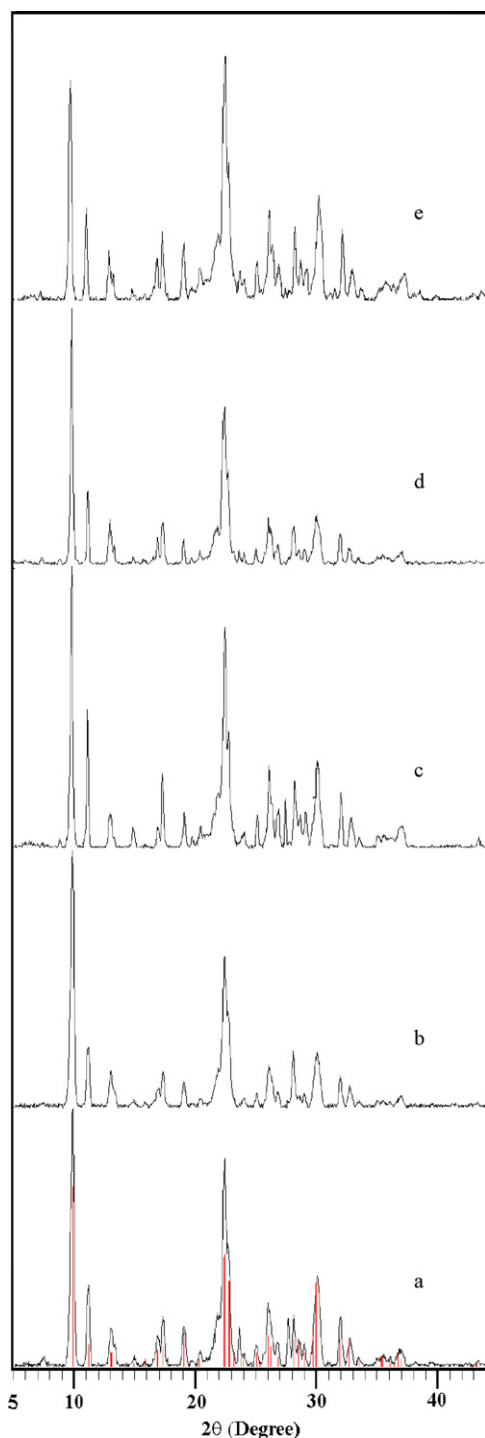


**Fig. 1.** XRD patterns of (a) the natural zeolite (Matched with reference pattern of clinoptilolite [25]) (b) Na (c) K and (d) Ca-exchanged form (e) clinoptilolite after zirconium adsorption (conditions: contact time = 24 h, Initial concentration = 0.01 mol L<sup>-1</sup>, Temperature = 40 °C and pH 1.0).

The XRD pattern of the natural zeolite and the reference pattern of clinoptilolite [25] are presented in Fig. 1a. It is obvious that clinoptilolite is the major phase in zeolite-rich rock examined. XRD patterns of the exchanged forms (Fig. 1b–e) are compared to that of the parent clinoptilolite. The lines, position and relative intensity remained intact.

The FTIR spectrum of clinoptilolite is presented in Fig. 2. The fact that zeolites are significantly hydrated is illustrated by the discrete water absorption bands in the 3500 and 1640 cm<sup>-1</sup> region. These

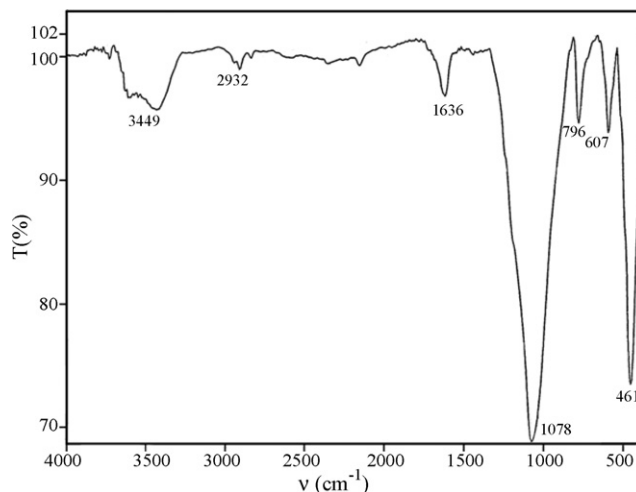


**Fig. 2.** FTIR spectrum of clinoptilolite.

bands, which were centered at 3449 and 1636 cm<sup>-1</sup>, refer to water molecules associated with Na and Ca in the channels and cages of the zeolite structure. As can be seen from the figure, other bands appear near the 1078 cm<sup>-1</sup> band arise from asymmetric stretching vibration modes of internal T–O bonds in TO<sub>4</sub> tetrahedra (T = Si and Al). The 799 and 471 cm<sup>-1</sup> bands are assigned to the stretching vibration modes of O–T–O groups and the bending vibration modes of T–O bonds, respectively [26,27].

The chemical composition of the zeolite samples obtained by XRF method is shown in Table 1. The Si/Al ratio of natural clinoptilolite was 5.086. Different Si/Al ratios have been reported for clinoptilolite but all of them are within the range (4–5.5) [17]. In this work the lowest Si/Al ratios of 4.88 was obtained for Ca-form.

In TG and DTG curves of the natural sample (Fig. 3a) a characteristic dehydration peak between 25 and 200 °C with 13.1% weight loss was observed. In zirconium exchanged zeolite a new dehydration peak was observed around 300 °C. It is suggested the water molecules bonded to zirconium are released at this temperature. The total weight loss in this sample is 18% (Fig. 3b)

### 3.2. Effect of contact time

The effect of contact time on zirconium adsorption was studied in zirconium solution of 0.01 mol L<sup>-1</sup> and mass-to-volume ratio of 1:20 at 30 °C. The initial pH was 1.85. The results are shown in Fig. 4. In all cationic forms, the equilibration was attained after 24 h. From the slope of the curves, it was concluded that adsorption rate was fast at the beginning and became slow with the progress of the reaction.

### 3.3. Effect of temperature

Adsorption capacities of different exchanged forms were measured at constant concentration of zirconium solution (0.01 mol L<sup>-1</sup>) and mass-to-volume ratio of 1:20 at four different temperatures (Fig. 5). Up to 40 °C, the adsorption capacity increased as the temperature increased. This could be attributed to the endothermic nature of the process. The calculated thermodynamic parameters (Table 3) reveal the endothermic nature of the reaction.

### 3.4. Adsorption kinetics and thermodynamics

The kinetics of adsorption was evaluated by applying four different models including the pseudo-first-order equation, the pseudo-second-order equation, Elovich equation and intra-particle

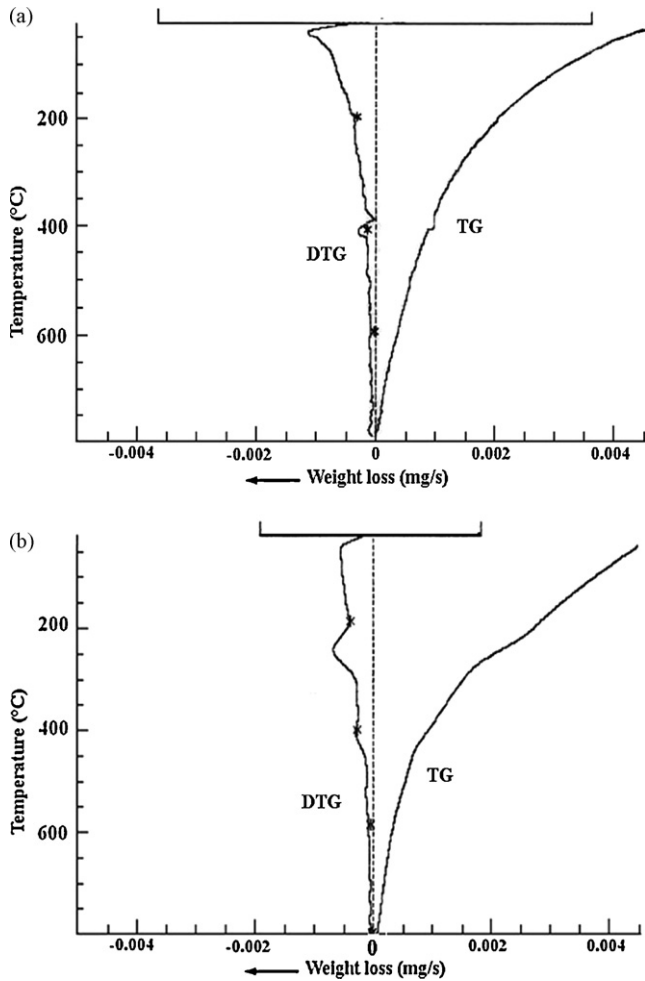


Fig. 3. TG and DTG curves of clinoptilolite (a) before and (b) after zirconium adsorption process (zirconium concentration = 0.01 mol L<sup>-1</sup>, temperature = 40 °C and contact time = 72 h).

diffusion model. These models were tested to fit experimental data obtained by batch experiments.

The pseudo-first-order equation is generally expressed as follows:

$$\frac{dq}{dt} = K_1(q_e - q_t) \quad (2)$$

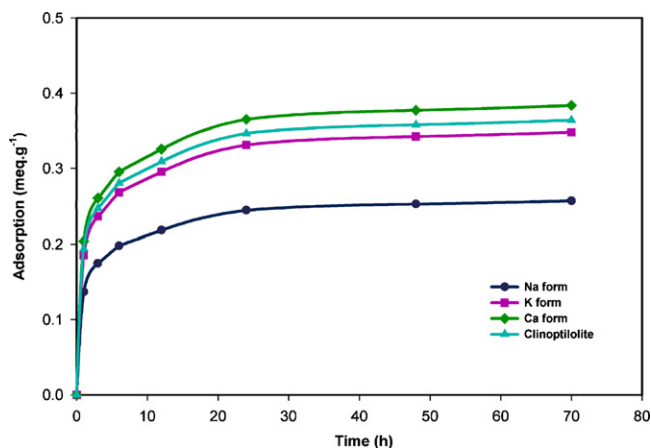


Fig. 4. Effect of contact time on zirconium adsorption (zirconium concentration = 0.01 mol L<sup>-1</sup>, temperature = 40 °C and pH 1.85).

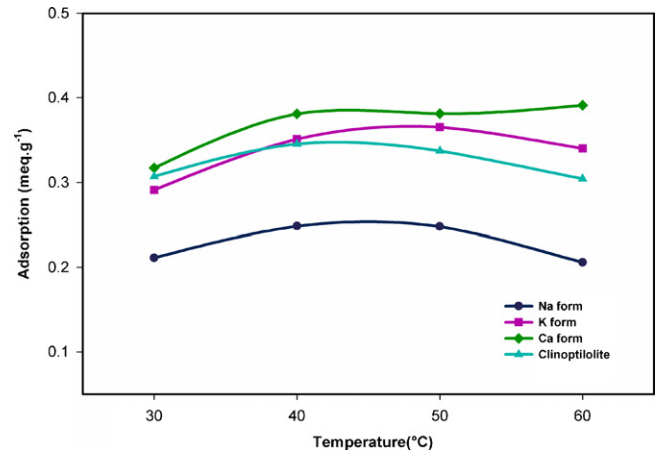


Fig. 5. Effect of temperature on zirconium adsorption (zirconium concentration = 0.01 mol L<sup>-1</sup>, contact time = 24 h and pH 1.85).

where  $q_e$  and  $q_t$  are the amount of species adsorbed per unit mass of sorbent at equilibrium and at any time  $t$ , respectively ( $\text{mmol g}^{-1}$ ) and  $K_1$  is the rate constant of pseudo-first-order sorption ( $\text{min}^{-1}$ ). After integration and applying boundary conditions, for  $t=0, q=0$ , the integrated form of equation becomes:

$$\ln(q_e - q_t) = \ln q_e - K_1 t \quad (3)$$

The pseudo-second-order equation based on adsorption equilibrium capacity can be expressed as:

$$\frac{dq}{dt} = K_2(q_e - q_t)^2 \quad (4)$$

where  $K_2$  is the rate constant of pseudo-second-order sorption ( $\text{g mmol}^{-1} \text{min}^{-1}$ ). Integrating this equation and applying boundary conditions for  $t=0, q=0$  gives:

$$\frac{t}{q_t} = \frac{1}{K_2 q_e^2} + \frac{t}{q_e} \quad (5)$$

Sorption rate can be obtained from Eq. (5):

$$\frac{q_t}{t} = \frac{1}{\left(\frac{1}{K_2 q_e^2} + \frac{t}{q_e}\right)} \quad (6)$$

and the initial sorption rate,  $h$ , can be defined as

$$h = K_2 q_e^2 \quad (7)$$

So Eq. (6) can become

$$q_t = \frac{t}{\left(\frac{1}{h} + \frac{t}{q_e}\right)} \quad (8)$$

The initial sorption rate,  $h$  ( $\text{mmol g}^{-1} \text{min}^{-1}$ ), the equilibrium sorption capacity,  $q_e$ , and the pseudo-second-order rate constant,  $K_2$ , can be determined experimentally from slope and intercept of plotting of  $t/q_t$  against  $t$ .

Table 3

Thermodynamic parameters obtained for the zirconium adsorption on the natural and cation exchanged forms of clinoptilolite.

Zeolite	$E_a$ (kJ mol <sup>-1</sup> )	$\Delta H$ (kJ mol <sup>-1</sup> )	$\Delta S$ (kJ mol <sup>-1</sup> K <sup>-1</sup> )	$\Delta G_{298}$ (kJ mol <sup>-1</sup> )
Na-form	4.46	9.22	0.0469	-4.77
K-form	10.60	15.60	0.0720	-5.81
Ca-form	3.00	13.30	0.0656	-6.22
Clinoptilolite	7.61	6.44	0.0424	-6.18

**Table 4**  
Kinetic parameters obtained for the zirconium adsorption on the natural and cation exchanged forms of clinoptilolite (pseudo-first-order and pseudo-second-order models).

Zeolite	$q_{e(\text{exp.})} (\times 10^{-2})$ (mmol g <sup>-1</sup> )	Pseudo-first-order model			Pseudo-second-order model		
		$k_1 (\times 10^{-3})$ (min <sup>-1</sup> )	$q_{e(\text{theor.})} (\times 10^{-2})$ (mmol g <sup>-1</sup> )	$R^2$	$K_2 (\times 10^{-1})$ (g mmol <sup>-1</sup> min <sup>-1</sup> )	$q_e (\times 10^{-2})$ (mmol g <sup>-1</sup> )	$R^2$
Na-form	6.11	1.25	3.07	0.9137	1.60	6.51	0.9992
K-form	8.28	1.31	4.16	0.9087	1.96	8.81	0.9987
Ca-form	9.13	1.28	4.58	0.9205	2.45	9.71	0.9981
Clinoptilolite	8.66	1.30	4.35	0.9182	2.02	9.22	0.9990

**Table 5**  
Kinetic parameters obtained for the zirconium adsorption on the natural and cation exchanged forms of clinoptilolite (Elovich and intra-particle diffusion models).

Zeolite	Elovich model			Intra-particle diffusion model		
	$\alpha (\times 10^{-3})$ (mmol g <sup>-1</sup> min <sup>-1</sup> )	$\beta$ (g mmol <sup>-1</sup> )	$R^2$	$k_{\text{diff}} (\times 10^{-3})$ (mmol g <sup>-1</sup> min <sup>-1/2</sup> )	$C (\times 10^{-3})$ (mmol g <sup>-1</sup> )	$R^2$
Na-form	8.83	124.0	0.9951	1.40	15.5	0.8095
K-form	11.90	90.9	0.9945	1.90	21.0	0.8310
Ca-form	13.20	81.9	0.9937	2.10	23.1	0.8123
Clinoptilolite	12.40	86.9	0.9965	2.00	21.9	0.7912

The Elovich equation is given as follows:

$$q_t = \frac{\ln(\alpha\beta)}{\beta} + \frac{\ln t}{\beta} \quad (9)$$

where  $q_t$  is the sorption capacity at time  $t$ ,  $\alpha$  is the initial sorption rate of Elovich equation (mmol g<sup>-1</sup> min<sup>-1</sup>), and the parameter  $\beta$  is related to the extent of surface coverage and activation energy for chemisorption (g mmol<sup>-1</sup>). The constants can be obtained from the slope and intercept of a straight line of  $q_t$  versus  $\ln t$ . The intra-particle diffusion model is

$$q_t = K_{\text{diff}} t^{1/2} + C \quad (10)$$

where  $K_{\text{diff}}$  is the intra-particle diffusion rate constant (mmol g<sup>-1</sup> min<sup>-1/2</sup>),  $C$  is the intercept.

Kinetic parameters and correlation coefficients for four kinetic models of zirconium adsorption on the zeolite samples were calculated from corresponding plots and listed in Tables 4 and 5. The values of  $R^2$  of pseudo-second-order kinetic model are higher for all the exchanged forms.

The pseudo-second-order kinetic model selected as the best model to fit experimental data and was taken for evaluation of  $E_a$ . The  $K_2$  value obtained in this model is considered as a scale for the rate of the reactions which has a highest value for the Ca-exchanged form with the lowest Si/Al ratio (Table 1). This means that at the higher amount of Al, the more exchange sites are available for zirconium and the exchange is faster.

The activation energy of the adsorption ( $E_a$ ) is evaluated from the slope of  $\ln K_2$  (rate constant of pseudo-second-order sorption) versus  $1/T$  using Arrhenius equation (Fig. 6).

$$\ln K_2 = \ln A - \frac{E_a}{RT} \quad (11)$$

where  $K_2$  and  $A$  are the rate constant and temperature independent factor (g mmol<sup>-1</sup> min<sup>-1</sup>), respectively,  $E_a$  is the activation energy of the reaction of adsorption (J mol<sup>-1</sup>),  $R$  is the gas constant (8.314 J mol<sup>-1</sup> K<sup>-1</sup>) and  $T$  is the adsorption absolute temperature (K).

In order to obtain thermodynamic parameters, the distribution coefficient,  $k_d$  (mL g<sup>-1</sup>), value was determined according to equation;

$$k_d = \left( \frac{C_i - C_f}{C_i} \right) \times V/W \quad (12)$$

where  $C_i$  and  $C_f$  are respectively the initial and final concentrations of the zirconium in solution,  $W$  is the weight of zeolite (g) and  $V$  is the volume of the solution (mL).

The values of  $\Delta H^\circ$  and  $\Delta S^\circ$  were calculated from the slopes and intercepts of the linear variation of  $\ln K_d$  with the reciprocal of the temperature,  $1/T$  (Fig. 7).

$$\ln k_d = -(\Delta H^\circ/RT) + (\Delta S^\circ/R) \quad (13)$$

The free energy of the adsorption,  $\Delta G^\circ$  is calculated from:

$$\Delta G^\circ = \Delta H^\circ - T\Delta S^\circ \quad (14)$$

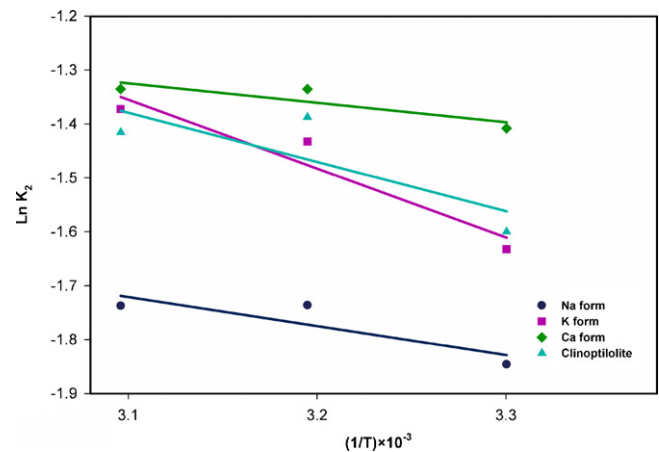


Fig. 6. Linear least square plots for obtaining  $E_a$ .

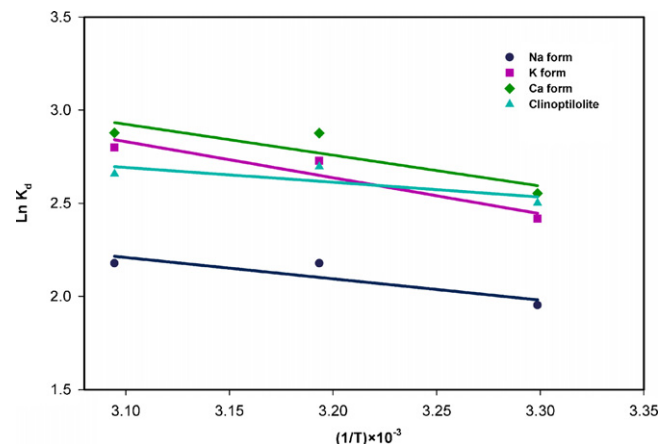


Fig. 7. Linear least square plots for obtaining thermodynamic parameters.

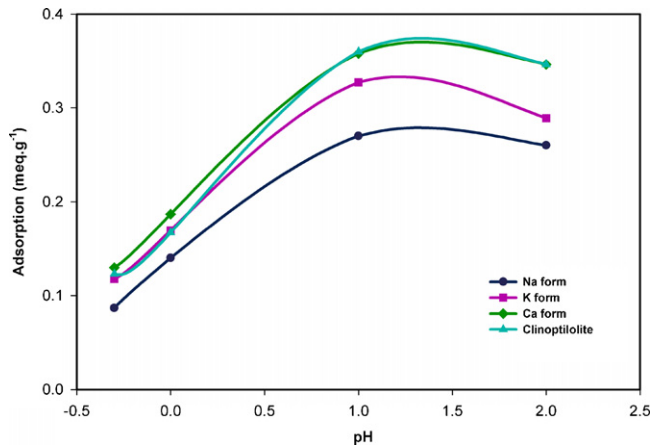


Fig. 8. Effect of pH on zirconium adsorption (zirconium concentration = 0.01 mol L<sup>-1</sup>, temperature = 40 °C and contact time = 24 h).

The activation energy and enthalpy values for all samples are positive. It means that adsorption of zirconium is an endothermic process. Lowest activation energy of adsorption belongs to Ca-form. Negative  $\Delta G^\circ$  values indicate that the adsorption process is favorable. The value for Ca-form is the highest and for Na-form is the lowest one.

### 3.5. Effect of initial pH

The concentration of zirconium species gradually change during the adsorption process. And the pH value of the solution depends on the concentration. Therefore the initial and final pH values were only measured and the effect of initial pH was studied. Maximum adsorption capacity at constant concentration of zirconium solution (0.01 mol L<sup>-1</sup>) and mass-to-volume ratio of 1:20 was obtained at pH 1 with slight decrease at pH 2 (Fig. 8). The higher pH values were not examined because of the precipitation of zirconium at pH > 2 [28]. In lower pHs, adsorption capacity decreased because H<sub>3</sub>O<sup>+</sup> acts as a competitive ion.

On the other hand, the reactions of zirconium in water are the subject of much controversy. Aqueous solution chemistry of zirconium and hydrolytic polymerization of aqueous zirconium ions are reported in several papers [29–34].

The onset of the hydrolysis of zirconium occurs in strongly acidic solution (pH < 0) and is dominated by the formation of polynuclear species. The onset of precipitation reactions also occurs at low pH (about 2). These features have made the hydrolysis and solubility of this cation difficult to study.

Walther et al. investigated polynuclear species of zirconium in acidic aqueous solution by combining X-ray absorption spectroscopy (XAFS) and nano-electrospray mass spectrometry (ESI-MS). Species distributions were measured at 0 < pH < 3 for [Zr] = 1.5–10 mmol L<sup>-1</sup>. While the monomer remains a minor species, with increasing pH the degree of polymerization increases and the formation of tetramers, pentamers, octamers, and larger polymers is observed [31].

It became evident that the Zr<sup>4+</sup> ion is stable only under very acidic conditions (pH < 0), and that mononuclear hydroxide complexes dominate only in very dilute solutions ([Zr] < 10<sup>-5</sup> mol L<sup>-1</sup>). At higher concentrations or lower acidities, the solvated Zr<sup>4+</sup> ion (Zr<sup>4+</sup>·8H<sub>2</sub>O) hydrolyzes and forms (Zr(OH)<sup>3+</sup>·7H<sub>2</sub>O) and (Zr(OH)<sub>2</sub><sup>2+</sup>·6H<sub>2</sub>O). The low adsorption capacity obtained for different forms is attributed to the formation of these species.

The distribution of hydrolyzed species of zirconium as a function of pH is shown in Fig. 9. Although it is difficult to define zirconium form in aqueous solution because of depending its species to pH and

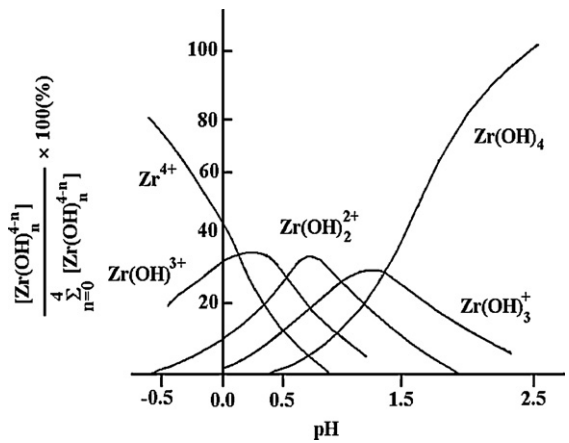


Fig. 9. Distribution of hydrolyzed species of zirconium as a function of pH.

concentration, but the best pH find to be 1 for adsorption of zirconium because at this pH zirconium is in various monomer forms (Zr<sup>4+</sup>, Zr(OH)<sup>3+</sup>, Zr(OH)<sub>2</sub><sup>2+</sup>, Zr(OH)<sub>3</sub><sup>+</sup> and Zr(OH)<sub>4</sub>).

### 3.6. Adsorption isotherms

Adsorption isotherms were plotted by the data obtained at different concentrations by the following equation (Fig. 10):

$$a = (C_i - C_e) \times V/m \quad (15)$$

$a$  is the amount of metal species adsorbed by unit mass of zeolite (mg g<sup>-1</sup>) at equilibrium;  $C_i$  and  $C_e$  are respectively the initial and equilibrium concentration of zirconium (mg L<sup>-1</sup>);  $m$  is the amount of zeolite (g) and  $V$  is the volume of zirconium solution (L). The value of  $a$  is valid for equilibrium at particular temperature (here 40 °C).

Two adsorption isotherm models were used for fitting of the experimental data. The Freundlich equation;

$$a = k_F C^n \quad (16)$$

was initially applied in its linear form

$$\ln a = \ln k_F + n \ln C \quad (17)$$

where  $k_F$  is the known Freundlich constant related to the adsorbent capacity and  $n$  is an exponent related to the strength of the adsorption. The applicability of the Langmuir equation was also tested, where Langmuir constant  $k_L$  and the saturation capacity  $a_m$  can be

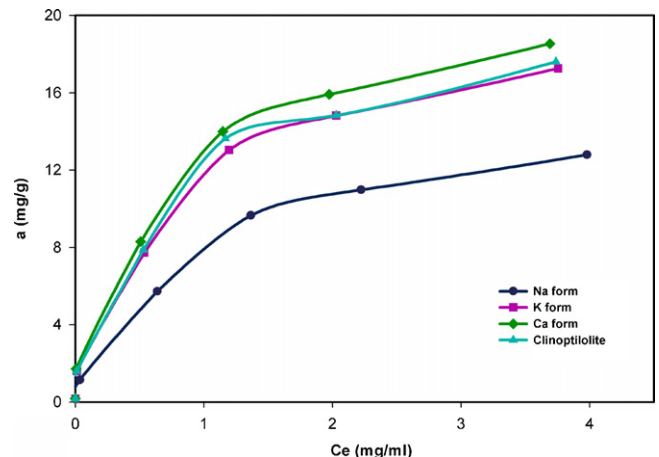


Fig. 10. Adsorption isotherms at 40 °C in optimum conditions.

**Table 6**  
Adsorption isotherm parameters for the zirconium onto natural and cation exchanged forms of clinoptilolite.

Zeolites	Langmuir			Freundlich		
	$k_L(\text{cm}^3 \text{mg}^{-1})$	$a_m(\mu\text{g g}^{-1})$	$R^2$	$K_F(\text{cm}^3 \text{g}^{-1})$	$n$	$R^2$
Na-form	10.14	6180	0.9989	1.4882	0.6116	0.9945
K-form	16.31	7990	0.9998	5.5656	0.5463	0.9862
Ca-form	88.43	8880	0.9986	16.5718	0.4758	0.9904
Natural	24.73	8312	0.9994	6.4405	0.5377	0.9890

evaluated by regression analysis of the linear forms of the following equation:

$$a = \frac{a_m k_L C}{(1 + k_L C)} \quad (18)$$

In particular we used the linear expression:

$$\frac{1}{a} = \frac{1}{a_m} + \frac{1}{a_m k_L} \times \frac{1}{C} \quad (19)$$

Figs. 11 and 12 show respectively the linearized Langmuir and Freundlich adsorption isotherms. The parameters for two isotherms obtained from experimental data and the related correlation coefficients ( $R^2$ ) are presented in Table 6. The Langmuir model yields better correlation coefficients. The applicability of the Langmuir isotherm suggests monolayer coverage of the zirconium species at the surface of the zeolite.  $n < 1$  obtained in Freundlich model depict a favorable adsorption. The smallest  $n$  value obtained for Ca-form means the better adsorption process.

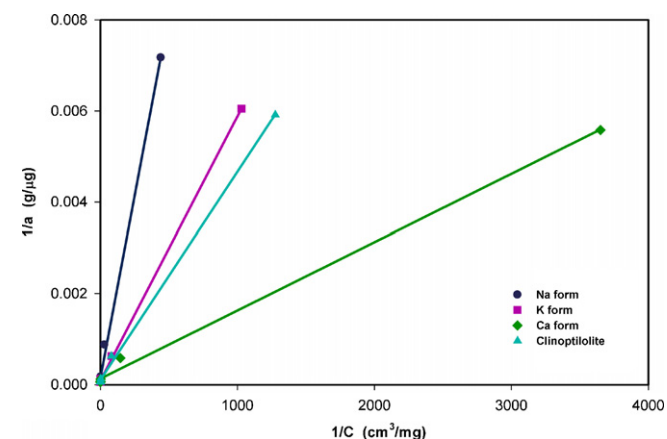


**Fig. 11.** Linear least square plots for calculating parameters of Langmuir isotherm.

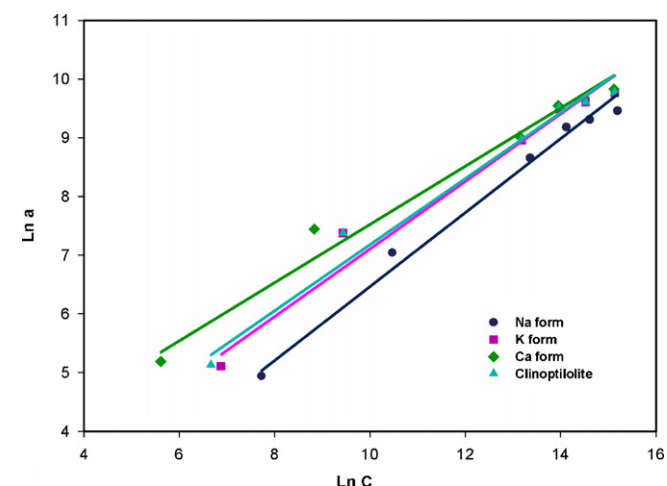


**Fig. 12.** Linear least square plots for calculating parameters of Freundlich isotherm.

## 4. Conclusions

Clinoptilolite is an abundant natural zeolite and highly stable against radioactive radiations. The adsorption capacity of  $0.4 \text{ meq g}^{-1}$  obtained for Ca-form of this zeolite make it a favorable candidate for Zr removal from high level radioactive liquid wastes. Among two applied isotherm models, Langmuir isotherm gave better correlation with the experimental data. Positive  $\Delta H^\circ$  and negative  $\Delta G^\circ$  indicated endothermic nature and feasibility of the adsorption process. Fitting data to kinetics models and values of  $R^2$  showed that the pseudo-second-order kinetic model is the best model for kinetics of zirconium adsorption.

## References

- [1] Y.Q. Zhang, R.S. Wang, C.Sh. Lin, X.Y. Zhang, Selective separation behavior of zirconium in simulated high level radioactive liquid waste, J. Radioanal. Nucl. Chem. 247 (2001) 205–208.
- [2] K. Akhtar, M.W. Akhtar, A.M. Khalid, Removal and recovery of zirconium from its aqueous solution by *Candida tropicalis*, J. Hazard. Mater. 156 (2008) 108–117.
- [3] F.L. Moore, Separation of zirconium from other elements by liquid-liquid extraction, Anal. Chem. 28 (1956) 997–1001.
- [4] X.J. Yang, C. Pin, Separation of hafnium and zirconium from Ti- and Fe-rich geological materials by extraction chromatography, Anal. Chem. 71 (1999) 1706–1711.
- [5] F.W.E. Strelow, Separation of zirconium from titanium, ferric iron, aluminum, and other cations by cation exchange chromatography, Anal. Chem. 31 (1959) 1974–1977.
- [6] J.S. Fritz, R.T. Frazee, Reversed-phase chromatographic separation of zirconium and hafnium, Anal. Chem. 37 (1965) 1358–1361.
- [7] M. Smolik, A. Jakóbk-Kolon, M. Porański, Separation of zirconium and hafnium using Diphonix® chelating ion-exchange resin, Hydrometallurgy 95 (2009) 350–353.
- [8] G.W.C. Milner, J.W. Edwards, The analytical chemistry of zirconium, Analyst 85 (1960) 86–97.
- [9] R.G. Dosch, F.J. Conrad, Cation exchange separation of titanium and zirconium using perchloric acid. Application to the analysis of PZT ceramics, Anal. Chem. 36 (1964) 2306–2308.
- [10] M. Qureshi, K. Husain, Quantitative cation exchange separation of zirconium and hafnium in formic acid media, Anal. Chem. 43 (1971) 447–449.
- [11] E.M. Larsen, P. Wang, The ion exchange of zirconium and hafnium in perchloric acid with Amberlite IR-120, J. Am. Chem. Soc. 76 (1954) 6223–6229.
- [12] X.J. Yang, A.G. Fane, C. Pin, Separation of zirconium and hafnium using hollow fibers – Part I. Supported liquid membranes, Chem. Eng. J. 88 (2002) 37–44.
- [13] X.J. Yang, A.G. Fane, C. Pin, Separation of zirconium and hafnium using hollow fibers – Part II. Membrane chromatography, Chem. Eng. J. 88 (2002) 45–51.
- [14] A. Dyer, F.H. Kadhim, Inorganic ion-exchangers for the removal of zirconium, hafnium and niobium radioisotopes from aqueous solutions, J. Radioanal. Nucl. Chem. 131 (1989) 161–169.
- [15] T. Maesen, The zeolite scene – An overview, in: J. Čejka, H. van Bekkum, A. Corma, F. Schüth (Eds.), Introduction to Zeolite Science and Practice, Studies in Surface Science and Catalysis, vol.168, third ed., Elsevier, Amsterdam, 2007, pp. 1–12.
- [16] O. Altin, H.Ö. Özbelge, T. Doğu, Use of general purpose adsorption isotherms for heavy metal-clay mineral interactions, J. Colloid Interface Sci. 198 (1998) 130–140.
- [17] D.W. Breck, Zeolite Molecular Sieves, Structure, Chemistry and Use, Wiley, New York, 1974.
- [18] G.M. Haggerty, R.S. Bowman, Sorption of chromate and other inorganic anions by organo-zeolite, Environ. Sci. Technol. 28 (1994) 452–458.
- [19] G. Cerri, A. Langella, M. Pansini, P. Cappelletti, Methods of determining cation exchange capacities for clinoptilolite-rich rocks of the Logudoro region in Northern Sardinia, Italy, Clays Clay Miner. 50 (2002) 127–135.
- [20] R.T. Pabalan, Thermodynamics of ion-exchange between clinoptilolite and aqueous solutions of  $\text{Na}^+/\text{K}^+$  and  $\text{Na}^+/\text{Ca}^{2+}$ , Geochim. Cosmochim. Acta 58 (1994) 4573–4590.
- [21] M.J. Semmens, W.P. Martin, The influence of pretreatment on the capacity and selectivity of clinoptilolite for metal ions, Water Res. 22 (1988) 537–542.

- [22] M.A. Stylianou, V.J. Inglezakis, K.G. Moustakas, S.P. Malamis, M.D. Loizidou, Removal of Cu(II) in fixed bed and batch reactors using natural zeolite and exfoliated vermiculite as adsorbents, *Desalination* 215 (2007) 133–142.
- [23] S. Capasso, E. Coppola, P. Iovino, S. Salvestrini, C. Colella, Sorption of humic acids on zeolitic tuffs, *Microporous Mesoporous Mater.* 105 (2007) 324–328.
- [24] S.K. Alpat, O. Ozbayrak, S. Alpat, H. Akcay, The adsorption kinetics and removal of cationic dye, Toluidine Blue O, from aqueous solution with Turkish zeolite, *J. Hazard. Mater.* 151 (2008) 213–220.
- [25] M.M.J. Treacy, J.B. Higgins, *Collection of Simulated XRD Powder Patterns for Zeolites*, Fifth ed., Elsevier, Amsterdam, 2007.
- [26] H. Tanaka, N. Yamasaki, M. Muratani, R. Hino, Structure and formation process of (K,Na)-clinoptilolite, *Mater. Res. Bull.* 38 (2003) 713–722.
- [27] M.J. Wilson, *Clay Mineralogy: Spectroscopic and Chemical Determinative Methods*, Chapman & Hall, New York, 1994.
- [28] G.Y. Guo, Y.L. Chen, W.J. Ying, Thermal, spectroscopic and X-ray diffractational analyses of zirconium hydroxides precipitated at low pH values, *Mater. Chem. Phys.* 84 (2004) 308–314.
- [29] R.E. Connick, W.H. McVey, The aqueous chemistry of zirconium, *J. Am. Chem. Soc.* 71 (1949) 3182–3191.
- [30] J.J. Tulock, G.J. Blanchard, Investigating hydrolytic polymerization of aqueous zirconium ions using the fluorescent probe pyrenecarboxylic acid, *J. Phys. Chem. B* 106 (2002) 3568–3575.
- [31] C. Walther, J. Rothe, M. Fuss, S. Büchner, S. Koltsov, T. Bergmann, Investigation of polynuclear Zr(IV) hydroxide complexes by nanoelectrospray mass-spectrometry combined with XAFS, *Anal. Bioanal. Chem.* 388 (2007) 409–431.
- [32] R.E. Connick, W.H. Reas, The hydrolysis and polymerization of zirconium in perchloric acid solution, *J. Am. Chem. Soc.* 73 (1951) 1171–1176.
- [33] A. Singhal, L.M. Toth, J.S. Lin, K. Affholter, Zirconium (IV) tetramer/octamer hydrolysis equilibrium in aqueous hydrochloric acid solution, *J. Am. Chem. Soc.* 118 (1996) 11529–11534.
- [34] C. Ekberg, G. Källvenius, Y. Albinsson, P.L. Brown, Studies on the hydrolytic behavior of zirconium (IV), *J. Solution Chem.* 33 (2004) 47–79.